Journal of Power Sources 189 (2009) 467–470

Contents lists available at ScienceDirect

Journal of Power Sources

journal homepage: www.elsevier.com/locate/jpowsour

Short communication

Preparation and performance of novel Li–Ti–Si–P–O–N thin-film electrolyte for thin-film lithium batteries

Feng Wu[a,b], Yadong Liu[a], Renjie Chen[a,b,*], Shi Chen[a,b], Guoqing Wang[a,b]

[a] School of Chemical Engineering and the Environment, Beijing Key Laboratory of Environmental Science and Engineering, Beijing Institute of Technology, Beijing 100081, China
[b] National Development Center for High Technology Green Materials, Beijing 100081, China

ARTICLE INFO

Article history:
Received 5 August 2008
Received in revised form 30 October 2008
Accepted 11 December 2008
Available online 24 December 2008

Keywords:
Thin-film lithium battery
Solid electrolyte
Li–Ti–Si–P–O–N
Conductivity
Magnetron sputtering

ABSTRACT

Novel Li–Ti–Si–P–O–N thin-film electrolyte was successfully fabricated by RF magnetron sputtering from a Li–Ti–Si–P–O target in N_2 atmosphere at various temperatures. XRD, SEM, EDX, XPS, and EIS were employed to characterize their structure, morphology, composition and electrochemical performances. The films were smooth, dense, uniform, without cracks or voids, and possessed an amorphous structure. Their room temperature lithium-ion conductivities were measured to be from 3.6×10^{-7} S cm^{-1} to 9.2×10^{-6} S cm^{-1}, and the temperature dependence of the ionic conductivities fits the Arrhenius relation. This kind of electrolyte possessed good properties is a promising candidate material for solid-state thin-film lithium batteries.

1. Introduction

With the development of the micro-electronic industry, the micro-power sources are more and more strongly demanded [1–4]. Thin-film lithium batteries are the most powerful candidate due to its excellent advantages, i.e., high specific energy, long cycle life, good safe performance and environmental friendliness [5,6]. One of the key materials for this device is a lithium-ion conductor, which acts as a solid electrolyte [7]. Recently, although lithium phosphorous oxynitride (LiPON) is widely used as a solid electrolyte for thin-film lithium batteries [8–12], researchers have continued their research into new thin-film electrolytes due to their high ionic conductivities [13–18]. The NASICON-structured material $LiTi_2(PO_4)_3$ exhibits high ionic conductivity of about 10^{-6} S cm^{-1} at 25 °C, which can be further improved by Si^{4+} ion substitution for P^{5+} corresponding with the increasing Li^+ ion concentration [19]. The prospects of using this kind of electrolyte with high ionic conductivity in thin-film lithium battery systems are very attractive.

Generally, solid thin-film electrolytes have mainly been prepared through vacuum evaporation [11], RF sputtering [8,9,17,18], pulsed laser deposition [10,15,16], etc. The RF sputtering deposition method has developed rapidly over the last decades to the point where it has become established as the process of choice for the deposition of a wide range of industrially important coatings. In many cases, magnetron sputtered films now outperform films deposited by other physical vapor deposition (PVD) processes, and can over the same functionality as much thicker films produced by other surface coating techniques [20].

In this work, the nitrided Si-substituted $LiTi_2(PO_4)_3$ is prepared into thin-film by sputtering method, and its performances as electrolyte have been investigated.

2. Experimental

2.1. Preparation of target

The Li–Ti–Si–P–O target was prepared with a conventional cold press method. A mixture consisting of reagent grade Li_2CO_3, SiO_2, TiO_2, and $NH_4H_2PO_4$ (1.3:0.6:4:5.4 in mole%, with an 50% excess of Li_2CO_3 to compensate for the Li loss in heating and sputtering) was heated up to 700 °C and kept for 2 h. Then it was ball-milled and pressed into a 60-mm-diameter target and sintered at 900 °C for 5 h.

2.2. Preparation of thin films

The Li–Ti–Si–P–O–N thin films were deposited by RF magnetron sputtering from the Li–Ti–Si–P–O target in pure N_2 atmosphere. The base pressure was 1×10^{-5} Pa, which can guarantee the cleanness of the sputtering chamber. The working pressure was 1.0 Pa and

* Corresponding author at: School of Chemical Engineering and the Environment, Beijing Key Laboratory of Environmental Science and Engineering, Beijing Institute of Technology, Beijing 100081, China. Tel.: +86 10 68912508; fax: +86 10 68451429.
E-mail address: chenrj@bit.edu.cn (R. Chen).

0378-7753/$ – see front matter © 2008 Elsevier B.V. All rights reserved.
doi:10.1016/j.jpowsour.2008.12.042

the RF power was 120 W. The deposition temperatures were room temperature, 200 °C, 300 °C, 400 °C and 500 °C, respectively. For the measurement of electrochemical properties, a sandwich structure consisting of a layer of stainless steel (SS), a layer of thin-film electrolyte, another layer of stainless steel deposited successively was formed in a Si-wafer substrate. And the thin-film electrolytes were also fabricated in Si-wafer and stainless steel sheet substrate to perform the SEM observation, EDX analysis, XPS and XRD measurement, respectively.

As comparisons, non-nitrided Li–Ti–Si–P–O thin-film electrolytes were also fabricated in Ar atmosphere with the same other conditions.

2.3. Characterization of properties

XRD analysis (Rigaku Dmax-2400, CuKa radiation) was employed to determine the structure of the target and thin-film. The surface and cross-section micro-morphology of the thin-film electrolyte was observed using JSM-35C SEM photographer, in which the EDX analysis was also carried on. The XPS investigations were carried out (MK II, VG) using monochromatic AlKα radiation ($h\nu$ = 1486.6 eV). Electrochemical tests were performed using the sandwiched structure of SS/thin-film electrolyte/SS in CHI 660a. The electrochemical impedance spectroscopy was carried out in the frequency region of 1 Hz to 100 kHz, and simulated and analyzed by the software *ZsimpWin*.

3. Results and discussion

3.1. Analysis of impedance properties

The impedance spectra of non-nitrided Li–Ti–Si–P–O thin-film electrolyte prepared in Ar atmosphere is quite different from that of the nitrided thin-film electrolyte prepared in pure N_2, as shown in Fig. 1. There is an imperfect semicircle without a tail in the Nyquist plot of the non-nitrided film (Fig. 1(a)), and further measurements reviewed that the diameter of the semi-circle increases with temperature, which indicate that the conductivity of the non-nitrided thin-film electrolyte is not ionic conductivity but electronic conductivity. So the non-nitrided thin film can hardly be used as electrolyte for the thin-film lithium batteries. While the impedance spectrum of the nitride film electrolyte (Fig. 1(b)), consisting of a high frequency depressed semi-circle caused by bulk Li–Ti–Si–P–O–N film and a low frequency sloping line ascribed to the interfaces between film and adjacent SS electrodes, is characteristic of a thin-film conducting dielectric with bulk relaxation processes which sandwiched between blocking contacts. The equivalent circuit using the Cole–Cole Model [21] can be seen in the inset of Fig. 1, where Z_b (Constant Phase Element, CPE) represents the impedance of the blocked electrodes of SS, and Z_{el} (CPE) parallel with R_{el} represents the bulk electrolyte. This circuit can well accord with the impedance of the sandwich structure.

The reason why electrochemical properties of nitrided films are different from non-nitrided ones may be the followings: (i) substitution of the P–O bond with more covalent P–N bond decreases the electrostatic energy, which is helpful to the Li^+ conducting; (ii) the nitrogen atoms stabilize the mixed $P(O,N)_4$ tetrahedra through the delocalization of the π-bond [22]; (iii) Li^+ concentration increases after O^{2-} substitute by N^{3-}, which can be confirmed by the result of XPS (The composition of film before and after nitridation was $Li_{0.55}Ti_2Si_{0.31}P_{3.8}O_{14.2}$ and $Li_{0.89}Ti_2Si_{0.32}P_{3.8}O_{10.9}N_{2.52}$ separately.); (iv) substitution of –O– and =O with >N– and =N– (as shown in Fig. 7) forms more cross-linked structures in the process of nitridation, which may improve the performance of lithium-ion conduction. From this result, we can inferred that the nitridation of the thin-film improves the electrochemical stability, and the conductivity changes from electronic to ionic, so that it has prospect to be used as electrolyte for the thin-film lithium batteries.

The ionic conductivity σ of Li–Ti–Si–P–O–N films can be obtained by following equation:

$$\sigma = \frac{d}{RA} \tag{1}$$

where d is the film thickness, A the area of the SS contact, and R the film resistance, which can be estimated from the measured impedance by selecting the value of Z' when $-Z''$ goes through a local minimum in the electrochemical impedance spectra [23]. Electrochemical impedance spectra of the Li–Si–Ti–P–O–N film measured at different temperatures are shown in Fig. 2, from which we can see that the ionic conductivity increases with measured temperatures.

The temperature dependence of conductivities of the thin-film electrolytes is shown in Fig. 3. The conductivity σ of the thin-film

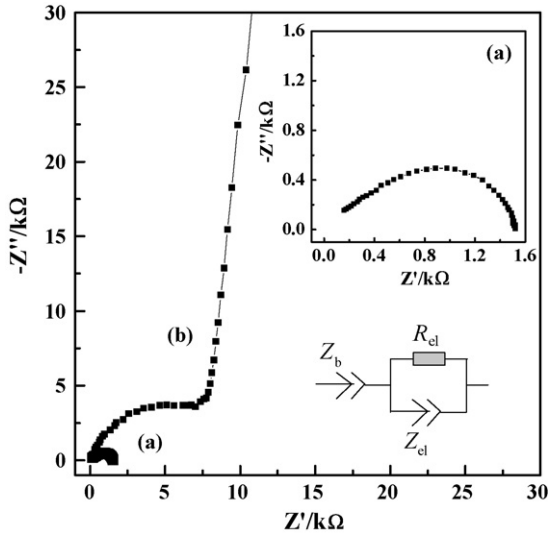

Fig. 1. Electrochemical impedance spectroscopy of the Li–Ti–Si–P–O (a) and Li–Ti–Si–P–O–N (b) thin films at room temperature.

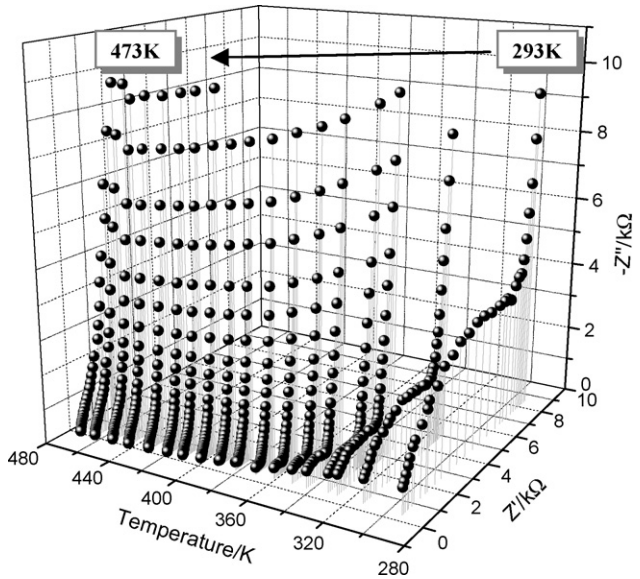

Fig. 2. Electrochemical impedance spectroscopy of the Li–Ti–Si–P–O–N thin-film measured in varies temperatures.

Table 1
The lithium-ion conductivities and active energies of film samples deposited in various temperatures.

Film samples	Deposition temperature (°C)	Ionic conductivity, σ (10^{-6} S cm^{-1})			Active energy, E (eV)
		25 °C	100 °C	200 °C	
A	89	0.36	4.6	45	0.37
B	200	2.3	27	180	0.33
C	300	4.3	53	270	0.32
D	400	8.4	70	410	0.29
E	500	9.2	75	420	0.29

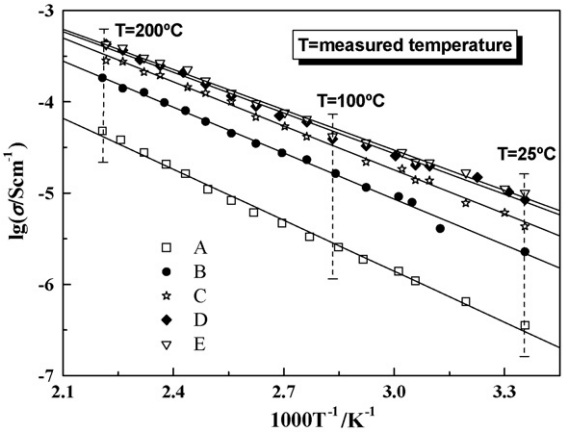

Fig. 3. Arrhenius plot of ionic conductivity of the Li–Ti–Si–P–O–N thin-film samples deposited in various temperatures.

electrolytes follow the Arrhenius equation:

$$\sigma = Ae^{[-E_\sigma/K_B T]} \quad (2)$$

where A is the pre-exponential factor, E_σ the activation energy of conduction, K_B the Boltzmann constant and T the absolute temperature. This proved that the thin-film electrolytes are good lithium-ion conductors. The ionic conductivities and conducting active energies of films deposited at different temperatures are shown in Table 1, in which we can see that the conductivity of the films increased with the increasing deposition temperatures but increased slower when the deposition temperature up to 500 °C. The room-temperature conductivity can reach 9.2×10^{-6} S cm^{-1}, and the corresponding activation energy of conduction E_σ is about 0.29 eV. This conductivity is larger than that of the well-known LiPON [8], but is much smaller than that of the bulk glass-ceramics [24]. The glass structure may be the main cause of why the conductivity was less than expected. So, further research maybe focus on annealing after deposition of the film to increase its ionic conductivity. However, this kind of amorphous electrolyte is still a competitive candidate to be used in thin-film lithium batteries.

3.2. Morphology and structure of the thin films

Fig. 4 shows the surface and cross-sectional view of the Li–Ti–Si–P–O–N thin-film prepared on Si-wafer substrate in 400 °C. As shown in Fig. 4(a), the surface of the film is smooth, dense, uniform, and without cracks or pinholes, which is very important for the thin-film electrolytes to avoid shortcut and safety problems. The thickness of the film measured from the cross-sectional SEM image of the film (Fig. 4(b)) was about 2.6 μm, which can be controlled by adjusting the sputtering time. From the Rutherford back-scattering spectroscopy (Fig. 4(c)) of the same film, we can see clearly the composition difference between layers. The composition of the thin-film estimated by the EDX spectroscopy as shown in Fig. 5 is approximately $Li_xTi_2Si_{0.32}P_{3.6}O_{7.16}N_{2.52}$, which was generally accord with the result of XPS. The EDX Spectroscopy

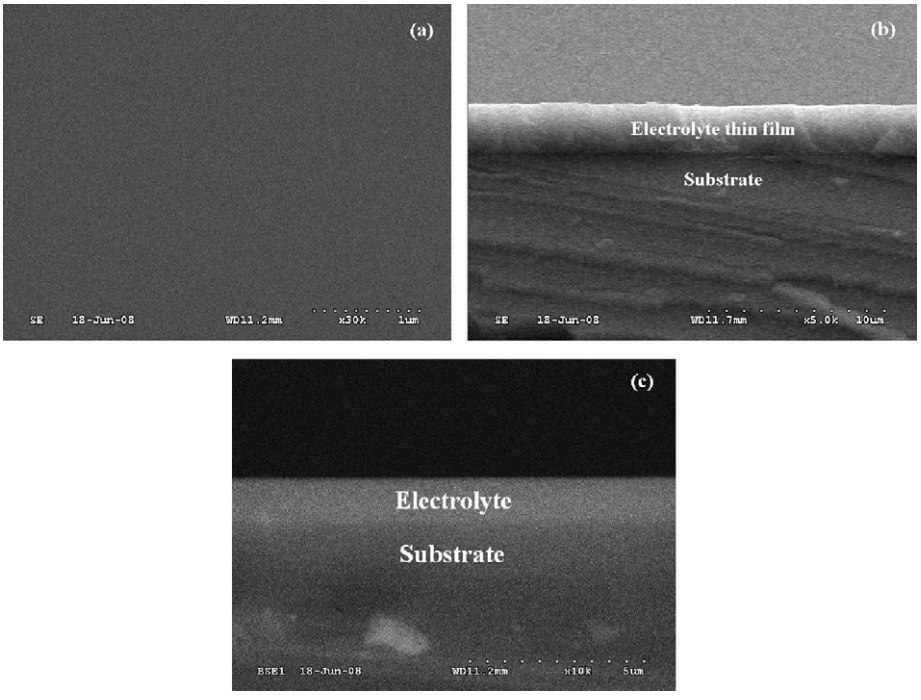

Fig. 4. SEM images of surface (a), cross-section (b) and RBS image of cross-section (c) of the Li–Si–Ti–P–O–N thin-film prepared in 400 °C.

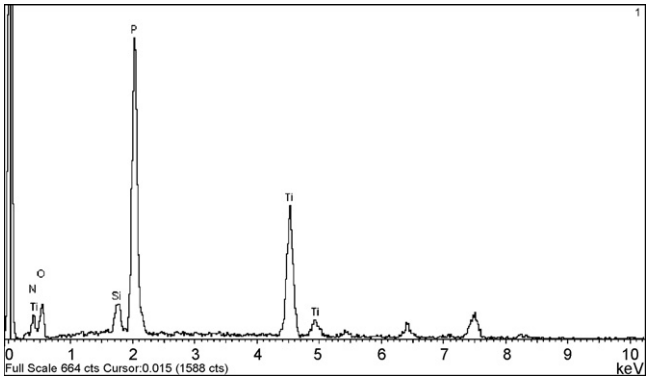

Fig. 5. EDX spectroscopy of the Li–Si–Ti–P–O–N thin films.

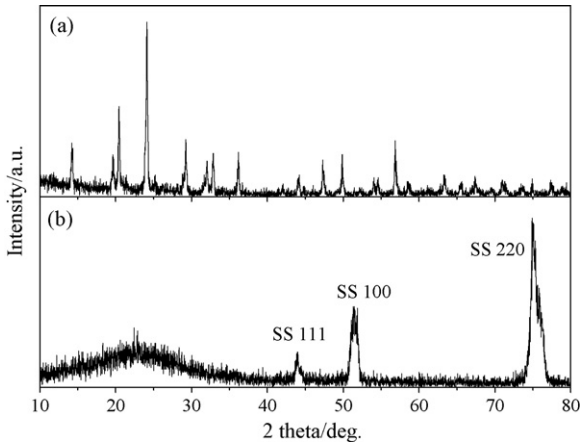

Fig. 6. XRD patterns of the Li–Si–Ti–P–O target (a) and the Li–Si–Ti–P–O–N thin-film deposited in 400 °C (b).

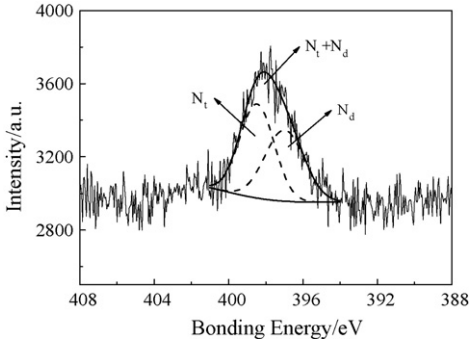

Fig. 7. XPS of the N 1 s region of the Li–Si–Ti–P–O–N thin-film deposited in 400 °C.

was measured in the structure of thin-film electrolyte deposited on stainless steel substrate. The unmarked peaks in the EDX spectroscopy can clearly be attributed to the stainless steel substrate consisting of Fe, Co, Ni and C.

Fig. 6(a) is the XRD pattern of the Li–Ti–Si–P–O target, which clearly shows the diffraction peaks due to the lithium-analogue of NASICON, i.e., $LiTi_2(PO_4)_3$, without any other impure phase. However, the XRD pattern for the thin-film electrolyte is devoid of any sharp peaks except that of the stainless steel substrate (i.e., 44° of SS(1 1 1), 51° of SS(1 0 0), 75° of SS(2 2 0)), from which we can demonstrate that the thin film has an amorphous structure.

From the N 1 s XPS spectrum (as shown in Fig. 7), the region of nitrogen contains two peaks originating from nitrogen having different chemical environments. The peak with lower binding energy (397.0 eV) comes from double-coordinated nitrogen –N═(N_d) bonded with P and Li^+ or Ti^{4+}. The triple-coordinated nitrogen from –N<(N_t) bonded with P or Si has higher binding energy (398.5 eV). More nitrogen, about 60%, is present in the form of N_t (Fig. 7). This result proved the incorporation of N into the thin film and formation of more cross-linked structure which may be beneficial for lithiumion conduction.

4. Conclusion

A kind of Li–Ti–Si–P–O–N thin-film electrolytes was fabricated by RF magnetron sputtering from a Li–Ti–Si–P–O target in pure N_2 atmosphere, which was not reported in literature. The films were smooth, dense, uniform, without cracks or pinholes, and possessed an amorphous structure. The room temperature ionic conductivities of the films increase with the deposition temperatures, which can reach about 9.2×10^{-6} S cm^{-1} and agree well with the Arrhenius equation. This kind of electrolytes exhibited good properties are promising candidate materials not only for solid-state thin-film lithium batteries, but also for thin-film electrochemical capacitors, micro-sensors, electrochromic devices and so on. Further works on improving the ionic conductivity by increasing the Li concentration in the thin film or changing configuration are in progress.

Acknowledgments

This work was financially supported by the National 973 Program (Contact Nos. 2002CB211800 and 2009CB220100), National High-tech 863 key program (Contact No. 2007AA03Z226).

References

[1] P.B. Koeneman, I.J. BuschVishniac, K.L. Wood, J. Microelectromech. Syst. 6 (1997) 355.
[2] J.N. Harb, R.M. LaFollette, R.H. Selfridge, L.L. Howelld, J. Power Sources 104 (2002) 46.
[3] S. Roundy, D. Steingart, L. Frechette, P. Wright, J. Rabaey, Wireless Sensor Networks 2920 (2004) 1.
[4] F. Albano, M.D. Chung, D. Blaauw, D.M. Sylvester, K.D. Wise, A.M. Sastry, J. Power Sources 170 (2007) 216.
[5] J.B. Bates, N.J. Dudney, B. Neudecker, A. Ueda, C.D. Evans, Solid State Ionics 135 (1995) 33.
[6] N.J. Dudney, B.J. Neudecker, Curr. Opin. Solid State Mater. Sci. 4 (1999) 479.
[7] V. Thangadurai, W. Weppner, Ionics 12 (2006) 81.
[8] J.B. Bates, N.J. Dudney, G.R. Gruzalski, R.A. Zuhr, A. Choudhury, C.F. Luck, J.D. Robertson, J. Power Sources 43 (1993) 103.
[9] J.B. Bates, N.J. Dudney, J. Power Sources 54 (1995) 58.
[10] B. Kim, Y.S. Cho, J.-G. Lee, K.-H. Joo, K.-O. Jung, J. Oh, B. Park, J.Y. Oh, J. Power Sources 109 (2002) 214.
[11] W.Y. Liu, Z.W. Fu, C.L. Li, Q.Z. Qin, Electrochem. Solid State Lett. 7 (2004) J36.
[12] F. Munoz, A. Duran, L. Pascual, L. Montagne, B. Revel, A.U.M. Rodrigues, Solid State Ionics 179 (2008) 574.
[13] X.M. Wu, X.H. Li, S.W. Wang, Z.O. Wang, Y.H. Zhang, M.F. Xu, Z.Q. He, Thin Solid Films 425 (2003) 103.
[14] S. Stramare, V. Thangadurai, W. Weppner, Chem. Mater. 15 (2003) 3974.
[15] J. Kawamura, N. Kuwata, K. Toribami, N. Sata, O. Kamishima, T. Hattori, Solid State Ionics 175 (2004) 273.
[16] J.K. Ahn, S.G. Yoon, Electrochem. Solid State Lett. 8 (2005) A75.
[17] J.M. Lee, S.H. Kim, Y. Tak, Y.S. Yoon, J. Power Sources 163 (2006) 173.
[18] Y.-D. Liu, F. Wu, R.-J. Chen, S. Chen, G.-Q. Wang, Trans. Beijing Inst. Technol. 27 (2007) 100.
[19] H. Aono, E. Sugimoto, Y. Sadaoka, N. Imanaka, G. Adachi, J. Electrochem. Soc. 137 (1990) 1023.
[20] P.J. Kelly, R.D. Arnell, Vacuum 56 (2000) 159.
[21] K.S. Cole, R.H. Cole, J. Chem. Phys. 9 (1941) 341.
[22] A. Le Sauze, R. Marchand, J. Non-Cryst. Solids 263 & 264 (2000) 285.
[23] X. Yu, J.B. Bates, G.E. Jellison, F.X. Hart, J. Electrochem. Soc. 144 (1997) 524.
[24] J. Fu, J. Mater. Sci. 33 (1998) 1549.